Blood First Edition Paper, prepublished online August 23, 2017; DOI 10.1182/blood-2017-01-760595

Molecular synergy underlies the co-occurrence patterns and phenotype of NPM1-mutant acute myeloid leukemia.

Oliver M Dovey[1], Jonathan L Cooper[1], Annalisa Mupo[1], Carolyn S Grove[1,3,4], Claire Lynn[5], , Nathalie Conte[6], Robert M Andrews[7], Suruchi Pacharne[1], Konstantinos Tzelepis[1], MS Vijayabaskar [1], Paul Green[1], Roland Rad[8], Mark Arends[9], Penny Wright[2], Kosuke Yusa[1], Allan Bradley[1], Ignacio Varela[10], and George S Vassiliou[1-2†].

[1]The Wellcome Trust Sanger Institute, Wellcome Trust Genome Campus, CB10 1SD, United Kingdom.

[2]Department of Haematology, Cambridge University Hospitals NHS Trust, Cambridge, UK.

[3]School of Pathology and Laboratory Medicine, University of Western Australia, Crawley, Western Australia, Australia.

[4]PathWest Division of Clinical Pathology, Queen Elizabeth II Medical Centre, Nedlands, Western Australia, Australia.

[5]Leukemia and Stem Cell Biology Group, Division of Cancer Studies, Department of Haematological Medicine, King's College London, Denmark Hill Campus, London SE5 9NU, UK.

[6]Sample Phenotype Ontology Team, The European Bioinformatics Institute, Wellcome Trust Genome Campus, CB10 1SD, United Kingdom.

[7]Institute of Translation, Innovation, Methodology and Engagement, Cardiff University School of Medicine, Heath Park, Cardiff, UK.

[8]Department of Medicine II, Klinikum Rechts der Isar, Technische Universität München, 81675 Munich, Germany; German Cancer Consortium (DKTK), German Cancer Research Center (DKFZ), 69120 Heidelberg, Germany.

[9]Cancer Research UK Edinburgh Centre, Institute of Genetics and Molecular Medicine, University of Edinburgh, Crewe Road, Edinburgh, UK.

[10]Instituto de Biomedicina y Biotecnología de Cantabria, Santander 39011, Spain.

†Correspondence: gsv20@sanger.ac.uk

Running Title: Molecular synergy in NPM1 mutant AML

Include article word count here: 3966

Abstract Word Count: 247

Scientific Category: Myeloid Neoplasia

Number of figures: 6

Number of references: 39

Key Points

- *Npm1c* and *Nras-G12D* co-mutation in mice leads to AML with a longer latency and a more mature phenotype than the *Npm1c/Flt3-ITD* combination
- Mutant *Flt3* or *Nras* allele amplification is the dominant mode of progression in *Npm1c/Flt3-ITD* and *Npm1c/Nras-G12D* murine AML

Abstract

NPM1 mutations define the commonest subgroup of acute myeloid leukemia (AML) and frequently co-occur with *FLT3* internal tandem duplications (ITD) or, less commonly, *NRAS* or *KRAS* mutations. Co-occurrence of mutant *NPM1* with *FLT3-ITD* carries a significantly worse prognosis than *NPM1-RAS* combinations. To understand the molecular basis of these observations we compare the effects of the two combinations on hematopoiesis and leukemogenesis in knock-in mice. Early effects of these mutations on hematopoiesis show that compound $Npm1^{cA/+};Nras^{G12D/+}$ or $Npm1^{cA};Flt3^{ITD}$ share a number of features: *Hox* gene over-expression, enhanced self-renewal, expansion of hematopoietic progenitors and myeloid differentiation bias. However, $Npm1^{cA};Flt3^{ITD}$ mutants, displayed significantly higher peripheral leucocyte counts, early depletion of common lymphoid progenitors and a monocytic bias compared to the granulocytic bias in $Npm1^{cA/+};Nras^{G12D/+}$ mutants. Underlying this was a striking molecular synergy manifested as a dramatically altered gene expression profile in $Npm1^{cA};Flt3^{ITD}$, but not $Npm1^{cA/+};Nras^{G12D/+}$, progenitors compared to wild type. Both double-mutant models developed high penetrance AML although latency was significantly longer with $Npm1^{cA/+};Nras^{G12D/+}$. During AML evolution, both models acquired additional copies of the mutant *Flt3* or *Nras* alleles, but only $Npm1^{cA/+};Nras^{G12D/+}$ mice showed acquisition of other human AML mutations, including *IDH1* R132Q. We also find, using primary Cas9-expressing AMLs, that *HoxA* genes and selected interactors or downstream targets are required for survival of both types of double-mutant AML. Our results show that molecular complementarity underlies the higher frequency and significantly worse prognosis associated with *NPM1*c/*FLT3-ITD* versus *NPM1/NRAS-G12D*-mutant AML and functionally confirm the role of HOXA genes in NPM1-driven AML.

[247 words]

Introduction

Advances in genomics have defined the somatic mutational landscape of acute myeloid leukemia (AML), leading to a detailed characterisation of their prognostic significance and patterns of mutual co-occurrence or exclusivity. [1,2] Mutations in *NPM1*, the gene for Nucleophosmin, characterise the most common subgroup of AML representing 25-30% of all cases, result in cytoplasmic dislocation of the protein (*NPM1c*) and are mutually exclusive of leukemogenic fusion genes.[1-3] As is often the case for fusion genes, progression to AML after the acquisition of mutant *NPM1* is contingent upon the gain of additional somatic mutations such as those that activate STAT and/or RAS signalling[3,4]. For reasons that are not clear, this transforming step favours acquisition of internal tandem duplications in *FLT3* (*FLT3*-ITD) over other somatic mutations with similar effects such as those involving *NRAS* or *KRAS*.[1-4] Furthermore, the *NPM1c/FLT3-ITD* combination is associated with a significantly worse prognosis compared to combinations of *NPM1c* with mutant *NRAS*, *KRAS* or other mutations.[2]

Whilst the adverse prognostic impact of *NPM1/FLT3-ITD* vs *NPM1/RAS* co-mutation influences clinical decisions in AML, its molecular basis and that of the frequent co-occurrence of *NPM1c* and *FLT3-ITD* in AML are unknown. Here, in order to investigate these phenomena, we compare the interaction of *Npm1c* with *Flt3-ITD* to its interaction with $Nras^{G12D}$ in knock-in mice. Individually, knock-in models of *NPM1c*, *FLT3-ITD* and *NRAS-G12D* display enhanced myelopoiesis and progression to myeloproliferative disorders or AML in a significant proportion of animals.[5-7] Also, we and others have previously shown that *Npm1c* and *Flt3-ITD* synergise to drive rapid-onset AML[8,9], but the interaction between *Npm1c* and mutant $Nras^{G12D}$ has not, to our knowledge, been previously investigated in knock-in mice[10]. Our findings reveal that the combination of *Npm1c* and *Flt3-ITD* has an early profound effect on gene expression and hematopoiesis, whilst *Npm1c* and *Nras-G12D* display only modest molecular synergy and subtler cellular changes. Also, whilst both types of co-mutation drove AML in the majority of mice, the leukemias in *Npm1c;Flt3-ITD* mice were more aggressive and undifferentiated than those which developed in *Npm1c;Nras-G12D animals*. At the genomic level, there was frequent amplification in both models of the mutant *Flt3-ITD* or *Nras-G12D* allele, however additional somatic mutations in AML driver genes (e.g. Idh1 and Ptpn11) were seen only in *Npm1c;Nras-G12D* AMLs. Our findings propose that the molecular synergy between *Npm1c* and *Flt3-ITD* underpin the co-occurrence patterns, phenotype and prognosis of NPM1-mutant AML.

Materials and methods

Animal husbandry

Mx1-Cre+;Npm1$^{flox\text{-}cA/+}$ were crossed with *Nras*$^{LSL\text{-}G12D}$ or *Flt3*^{ITD} mice, to generate triple transgenic animals (*Mx1-Cre;Npm1*$^{flox\text{-}cA/+}$*;Nras*$^{LSL\text{-}G12D/+}$ *and Mx1-Cre;Npm1*$^{flox\text{-}cA/+}$*;Flt3*$^{ITD/+}$). To activate conditional alleles (*Npm1*^{cA} and *Nras*^{G12D}) in approximately 12-14 week old *Mx1-Cre;Npm1*$^{flox\text{-}cA/+}$*;Nras*$^{LSL\text{-}G12D/+}$ mice, *Mx1-Cre* was induced by administration of pIpC. As described previously, *Mx-1 Cre;Npm1*$^{Flox\text{-}cA/+}$*;Flt3*$^{ITD/+}$ mutants do not require pIpC induction of *Mx1-Cre* and recombination of the *Npm1*$^{flox\text{-}cA}$ allele.[8] For pre-leukemic analyses *Npm1*$^{cA/+}$*;Nras*$^{G12D/+}$ were sacrificed 4-5 weeks post pIpC and *Npm1*$^{cA/+}$*;Flt3*$^{ITD/+}$ were sacrificed at 5 weeks of age. Genotyping for mutant alleles was performed as previously described.[5-7] All animal procedures were carried out in accordance with the Home Office Animals (Scientific Procedures) Act 1986 Amendment Regulations (2012) under project license 80/2564.

Hematological measurements

Blood counts were performed on a VetABC analyzer (Horiba ABX).

Histopathology

Formalin fixed, paraffin embedded (FFPE) sections were stained with hematoxylin and eosin. Samples from leukemic mice were also stained with anti-CD3, anti-B220 and anti-myeloperoxidase. All material was examined by two experienced histopathologists (P.W. and M.A.) blinded to mouse genotypes.

Colony-forming assays and serial re-plating

Nucleated cells (3 x10^4) from bone marrow (BM) aspirates of mutant and wild-type mice were suspended in cytokine-containing methylcellulose-based media (M3434, Stem Cell Technologies) and plated in duplicate wells of 6-well plates. Colony-forming units (CFUs) were counted 7 days later. For serial re-plating, 3 x10^4 cells were re-seeded and colonies counted after 7 days.

Flow cytometry and cell sorting

Single cell suspensions of BM cells or splenocytes were incubated in 0.85% NH_4Cl for 5 minutes to lyse erythrocytes. Cells were then suspended in Hank's Balanced Salt Solution (HBSS) supplemented with 2% FCS and 10µM HEPES. Progenitor populations were defined and stained as described in

supplementary methods. Gated cellularity was calculated by multiplying the percentage of gated cells by the total number of nucleated cells from BM samples after erythrocyte depletion.

Viral transduction of BM progenitors and AML cell culture.

Lineage depleted BM aspirates, isolated from wildtype and *Flt3*$^{ITD/+}$ mice, were transduced with MSCV-*Hoxa9*-GFP and/or MSCV-*Nkx2-3*-CFP retroviruses and expanded for 7 days in liquid culture (X-Vivo, Lonza, supplemented with 10ng/ml IL-3, 10ng/ml IL-6 and 50ng/ml SCF, Peprotech). CFP, GFP or double positive cells were FACS sorted and 2.5 x10^4 cells re-plated in semi-solid media as previously described. BM-derived AML cells from Roas26-EF1-Cas9 mice were cultured *in vitro* in the presence of cytokines. Disruption of individual candidate genes was performed by transduction with lentivirus expressing gene-specific guide RNA (gRNA) and blue fluorescent protein (BFP). The impact of gene disruption on AML cell growth was determined using competitive co-culture of transduced (BFP+) vs non-transduced (BFP-) cells as described previously[11] (Figure 6A, Supplemental methods).

Microarray and comparative genomic hybridization analysis

Mouse gene expression profiles (GEPs) were generated using the Illumina MouseWG-6 v2 Expression BeadChip platform (Illumina). DNA copy number variation in leukemic samples was assessed with Mouse Genome Comparative Genomic Hybridization 244K Microarray (acGH, Agilent Technologies). Full details of analysis are provided in supplemental methods. For mouse gene expression profiling, n=4-10 (Lin^-) or n=3-5 (MPP).

AML exome sequencing and mutation calling

Whole exome sequencing (WES) of AML BM and control C57BL/6N or 129Sv tail DNA was performed using the Agilent SureSelect Mouse Exon Kit (Agilent Technologies) and paired-end sequencing on a HiSeq2000 sequencer (Illumina). Validation of mutations was performed using MiSeq sequencing (Illumina) of amplicon libraries as previously described (See Supplemental Methods Figure S1 and Supplemental Tables 6 and 7 for primer sequences).[12,13] Full details of analysis are provided in supplemental methods.

Datasets

Microarray data were deposited at Array Express (accession number E-MTAB-5356), and RNA sequencing (accession numbers ERS1732539 to ERS1732546, ERS812461 and ERS812462) as well as exome and Miseq sequencing (accession numbers PRJEB18526 and ERP020464) at EBI ENA.

155

Results

Mutant *Npm1* co-operates with *Nras-G12D* and *Flt3-ITD* to increase self-renewal of hematopoietic progenitors and expand myelopoiesis

To understand the impact of the studied mutations, we analyzed hematopoietic cell compartments of $Npm1^{cA/+}$;$Nras^{G12D/+}$, $Npm1^{cA/+}$;$Flt3^{ITD/+}$, $Nras^{G12D/+}$, $Flt3^{ITD/+}$ and wild type (WT) mice 4-6 weeks after activation of conditional mutations (Figure 1). Compared to $Flt3^{ITD/+}$ single mutants, $Npm1^{cA/+}$;$Flt3^{ITD/+}$ mice displayed higher white cell counts (WCC) (56±13.4 vs 6.5±0.5 x10^6 g/L, p<0.001) and spleen weights (0.63g vs 0.16g, p<0.001), but not BM cellularity (Figure 1B). By contrast, both $Nras^{G12D/+}$ and $Npm1^{cA/+}$;$Nras^{G12D/+}$ mutants exhibited subtler increases in spleen weight (WT: 0.12g, $Nras^{G12D/+}$: 0.18g, $Npm1^{cA/+}$;$Nras^{G12D/+}$: 0.19g, p<0.01 and p<0.001 respectively), but increased BM cellularity (WT: 28.1±1.9 x10^6, $Nras^{G12D/+}$: 43.7±2.6 x 10^6 and $Npm1^{cA/+}$;$Nras^{G12D/+}$: 41.3±3.2 x10^6, p<0.01 for either comparison vs WT) (Figure 1B).

Expanded myelopoiesis and myeloproliferation were previously documented in single $Nras^{G12D/+}$ and $Flt3^{ITD/+}$ mutant mice.[5,6] Mutant *Npm1* augmented these phenotypes with increases in total Mac-1^+ splenocytes (from 27% to 50% for $Nras^{G12D/+}$; and 57% to 73% for $Flt3^{ITD/+}$). Notably, these cells were predominantly granulocytic (Mac-1^+/Gr-1^+) in $Npm1^{cA/+}$;$Nras^{G12D/+}$ and predominantly monocytic (Mac-1^+/Gr-1^-) in $Npm1^{cA/+}$;$Flt3^{ITD/+}$ mice (Supplemental Figure S1A).

$Nras^{G12D/+}$ mice have been shown to have increased hematopoietic stem (HSC) and progenitor cell numbers, due to increased proliferation and self-renewal of the HSC and multipotent progenitor (MPP) compartments.[14,15] Our results confirm these data demonstrating significant increases in total myeloid progenitors i.e. granulocyte-macrophage (GMP) and common-myeloid progenitors (CMP). Total numbers of Sca-1/Kit positive early progenitors (LSK) and MPPs are also increased in both $Npm1^{cA/+}$;$Nras^{G12D/+}$ and $Nras^{G12D/+}$ BM cells (Figure 1C and Supplemental Figure S2A). However, $Nras^{G12D/+}$ progenitor cell composition was largely unaltered by the addition of mutant NPM1. Concordant with previous studies, hematopoiesis in $Flt3^{ITD/+}$ mice was characterised by increased numbers of total myeloid progenitors (LK p<0.05 and GMPs p<0.01) and early progenitor populations (LSK, MPP and LMPP, p<0.01, p<0.01 and p<0.05 respectively) (Figure 1C and Supplemental Figure S2A). [16,17] Of note, there were detectable decreases in the size of the common lymphoid progenitor (CLP) population in $Flt3^{ITD/+}$ and $Npm1^{cA/+}$;$Flt3^{ITD/+}$ mice (Figure 1C) (in part due to the reduction in Il-7Rα-positive cells) (Figure S2B). $Npm1^{cA/+}$;$Flt3^{ITD/+}$ mice also exhibited robust increases in numbers of LK, LSK, MPP and LMPP populations, above what was observed with $Flt3^{ITD/+}$, when compared to WT. In direct comparison with $Flt3^{ITD/+}$ mutants, numbers of CMP and MEP

progenitors in $Npm1^{cA/+}$; $Flt3^{ITD/+}$ mice were reduced (from $55x10^3$ to $16x10^3$, $p<0.05$ and from $61x10^3$ to $17x10^3$, $p<0.05$), yet GMPs, proposed as direct descendants of CMPs[18], are significantly increased. This demonstrates that $Flt3^{ITD/+}$ mutant myelopoiesis is dramatically altered by the addition of $Npm1^{cA/+}$. In direct comparison with $Npm1^{cA/+}$;$Nras^{G12D/+}$, $Npm1^{cA/+}$;$Flt3^{ITD/+}$ mice showed increased LMPP and GMP populations with reduced numbers of lymphoid progenitors (CLP) (Figure 1E).

In order to assess the effects on the earliest detectable hematopoietic stem cell compartment (HSC) we opted to perform E-SLAM staining ($CD45^+/EPCR^+/CD48^-/CD150^+$).[19] Importantly, this does not rely on cell surface expression of FLT3, and reveals the percentage of E-SLAM detectable HSCs is decreased in $Npm1^{cA/+}$;$Nras^{G12D/+}$ mice and further so in $Npm1^{cA/+}$;$Flt3^{ITD/+}$mutants (Figure 1D). Finally, using serial re-plating of BM cells in semi-solid media we show that $Npm1^{cA/+}$ co-mutation markedly increased self-renewal of $Flt3^{ITD/+}$ (as shown previously [8]) and of $Nras^{G12D/+}$ cells (Figure 1F).

An *Npm1*$^{cA/+}$ transcriptional signature persists in double mutant hematopoietic progenitors

To examine their combined effects on transcription we performed comparative global gene expression profiling of lineage negative (Lin^-) BM cells using microarrays. $Npm1^{cA/+}$;$Nras^{G12D/+}$ and $Npm1^{cA/+}$;$Flt3^{ITD/+}$ cells displayed a dramatically altered GEP compared to single $Nras^{G12D/+}$ or $Flt3^{ITD/+}$ mutants (Figure 2A and Supplemental Figure S3B). Previously, we showed that mouse $Npm1^{cA/+}$ Lin^- cells overexpressed several homeobox *(Hox)* genes (in particular overexpression of *Hoxa5*, *Hoxa7*, *Hxa9* and two other homeobox genes, *Hopx* and *Nkx2-3*).[7] Here, we show that this signature, absent from $Nras^{G12D/+}$ or $Flt3^{ITD/+}$ singular mutant mice, persists in compound $Npm1^{cA/+}$;$Nras^{G12D/+}$ and $Npm1^{cA/+}$;$Flt3^{ITD/+}$ Lin^- progenitors. (Figure 2A, Supplemental Figure S3A-C). Gene Set Enrichment Analysis (GSEA) of $Npm1^{cA/+}$ single and compound mutant cell GEPs, showed significant enrichment for genes up-regulated in NPM1-mutant and *MLL*-fusion gene positive human leukemias (Figure 2A).

Overexpression of the homeobox gene NKX2.3 in human NPM1-mutant AML

Using the human TCGA AML dataset, we compared GEPs of NPM1 mutant ($NPM1c^{+ve}$) to NPM1 wildtype ($NPM1^{wt}$) AML.[1] In agreement with previously published analyses, both *HOXA* and *HOXB* genes were significantly overexpressed in $NPM1c^{+ve}$ AML (Figure 2B).[20] We also noted *NKX2-3* was also overexpressed in keeping with our findings in $Npm1^{cA/+}$ mice (Figure 2A). Recently, *NKX2-3* overexpression was shown to be the most effective discriminant of *MLL-MLLT4* (*MLL-AF6*)-driven AML from AMLs driven by other *MLL*-fusion genes. [21] Whilst overexpression of *Hox* genes such as *Hoxa9* has been shown to impart increased self-renewal and proliferation of hematopoietic progenitors, the effects of *Nkx2-3* overexpression are unknown. [22] To study this we performed retroviral gene transfer of fluorescently tagged *Nkx2-3*-CFP and *Hoxa9*-GFP into wildtype and $Flt3^{ITD/+}$

Lin$^-$ cells. Cells were subsequently sorted and plated in semi-solid methylcellulose for colony formation assays (Figure 2Ci). We find that overexpression of *Nkx2-3* increases clonogenic potential, albeit to a lesser extent compared to *Hoxa9* overexpression, in both wildtype and *Flt3*$^{ITD/+}$ progenitors. Notably, this is not augmented in combined transfected cells. (Figure 2Cii).

Hoxa gene expression is unaltered in mutant NPM1 early multipotent progenitors

In order to mitigate the impact of the studied driver mutations on cell surface phenotypes, we performed transcriptome analysis on a homogeneous population of early progenitors, purified LSK- MPPs, (Figure 2D). *Hox* gene expression was not significantly altered in this population in any of the *Npm1*$^{cA/+}$ models when compared to wildtype or single *Nras*$^{G12D/+}$ and *Flt3*$^{ITD/+}$ mutants (Figure 2E and Figure S3C). These results are in agreement with observations that *Hox* gene expression in human NPM1c AML blasts is comparable to that seen in WT human HSCs and myeloid progenitors.[20] As we do not observe statistically significant expansion in total (Lin$^-$) progenitors in single *Npm1*$^{cA/+}$ mice (figure 1C), these data propose that, unlike HSCs, the observed pattern of *Hox* overexpression in these progenitors is a molecular consequence of NPM1c rather than a change in cellular composition. This concurs with our published observations that the Hox signature is detectable even in CD19-positive B-cells[7].

MPPs from single *Nras*$^{G12D/+}$ or *Flt3*$^{ITD/+}$ and the respective *Npm1*$^{cA/+}$ compound mutant MPPs also had distinct transcriptional changes. Compared to WT, both *Nras*$^{G12D/+}$ and *Npm1*$^{cA/+}$;*Nras*$^{G12D/+}$ MPPs displayed small numbers of differentially expressed genes yet only ~20% of these were shared (Figure 2Di). GSEA did not uncover significant overlap with any pre-established expression signatures (data not shown). In contrast, the "addition" of *Npm1*$^{cA/+}$ to *Flt3*$^{ITD/+}$ in MPPs led to differential expression of a large number of additional genes, whilst also retaining most of the transcriptional changes attributable to *Flt3*$^{ITD/+}$ (Figure 2Dii, Table S2) demonstrating the powerful synergy between *Npm1*$^{cA/+}$ and *Flt3*$^{ITD/+}$. Pathway analysis of genes differentially expressed in *Npm1*$^{cA/+}$;*Flt3*$^{ITD/+}$ MPPs revealed enrichment of genes in the JAK-STAT pathway (Supplemental Figure 3E, Supplemental Tables S4), including the negative regulators *Cish* and *Socs2* (Figure 2F). A number genes, encoding proteins involved in MAPK signaling were also deregulated, as were genes involved in chromatin regulation/organisation and hematopoietic/myeloid differentiation (Figure 2F, Supplemental Figure 3D). Many of the genes in our *Npm1*$^{cA/+}$;*Flt3*$^{ITD/+}$ dataset were also found deregulated in a recently published Tet2$^{-/-}$;*Flt3*$^{ITD/+}$ mouse model of AML (, Supplemental Figure 3F and Supplemental Table 6,) which serves to verify our mouse dataset technically, but also reveals a distinguishing expression signature of FLT3-ITD which includes *Socs2*, *Id1*, *Csfr3r* and *Bcl11a*.[17] In contrast a lack of correlation

between deregulated gene sets of *Npm1*$^{cA/+}$;*Flt3*$^{ITD/+}$ and *Npm1*$^{cA/+}$;*Nras*$^{G12D/+}$ MPPs (Supplemental Figure S3D) emphasises the molecular distinction between these compound mutants.

Npm1$^{cA/+}$ and _Nras_^{G12D} collaborate to promote high penetrance AML

To understand the leukemogenic potential of combined *Npm1*$^{cA/+}$ and *Nras*^{G12D} mutations, we aged combined and single mutant cohorts. Compound *Npm1*$^{cA/+}$;*Nras*$^{G12D/+}$ and *Npm1*$^{cA/+}$;*Flt3*$^{ITD/+}$ mice had significantly reduced survival (median 138 and 52.5 days respectively) when compared to wildtype (618 days), *Npm1*$^{cA/+}$ (427 days), *Nras*$^{G12D/+}$ (315 days) and *Flt3*$^{ITD/+}$ (also 315 days) (Figure 3A, Supplemental Figure S4A). No difference in the survival of *Nras*$^{G12D/+}$ and *Flt3*$^{ITD/+}$ mutant mice was observed (p=0.85, see Supplemental Figure S4A for all comparisons). At time of sacrifice, blood counts and tissues were collected and subjected to histopathological analysis. Aged *Npm1*$^{cA/+}$;*Nras*$^{G12D/+}$ and *Npm1*$^{cA/+}$;*Flt3*$^{ITD/+}$ mice exhibited characteristic AML pathological findings at a much higher frequency than single mutant mice. These included significantly higher WCC, reduced platelet numbers and substantial organ infiltration with leukemic cells (Supplemental Figure S4B-D). Histological analysis verified the increased AML incidence from 41% (*Flt3*$^{ITD/+}$) to 100% in *Npm1*$^{cA/+}$;*Flt3*$^{ITD/+}$ samples and from 13% (*Nras*$^{G12D/+}$) to 85% in *Npm1*$^{cA/+}$;*Nras*$^{G12D/+}$ samples (45% AML with maturation, AML^{+} and 40% AML without maturation, AML^{-} as defined by the Bethesda classification[23] (Figure 3B).

Additional somatic mutations are required for progression to AML in _Npm1_$^{cA/+}$; _Nras_$^{G12D/+}$ mice.

Npm1$^{cA/+}$;*Flt3*$^{ITD/+}$ mice succumb to AML significantly more rapidly, compared to *Npm1*$^{cA/+}$ and *Npm1*$^{cA/+}$;*Nras*$^{G12D/+}$mice. We hypothesised that the slower onset of AML in the latter two genotypes may be due to the requirement for additional cooperating mutations. To test this, we performed aCGH and WES of AMLs from *Npm1*$^{cA/+}$, *Npm1*$^{cA/+}$;*Flt3*$^{ITD/+}$and *Npm1*$^{cA/+}$;*Nras*$^{G12D/+}$ mice. We first confirmed the frequent development of loss-of-heterozygosity (LOH) at the *Flt3* locus in *Npm1*$^{cA/+}$;*Flt3*$^{ITD/+}$ AMLs [8,24] and verified this by quantifying *Flt3*^{ITD} variant allele fractions (VAFs) using PCR-MiSeq (Figure 4Ai). aCGH showed that LOH was copy-neutral and due to uniparental disomy of *Flt3*^{ITD} (Supplementary Figure 4Aii). Interestingly, aCGH of *Npm1*$^{cA/+}$;*Nras*$^{G12D/+}$ samples revealed amplification of chr3 in 5/10 samples tested (Figure 4Bi). This was exclusive to *Npm1*$^{cA/+}$;*Nras*$^{G12D/+}$ AMLs and mapped to a minimally amplified region (chr3: 102743581-103470550) containing *Nras* (Supplementary Table S10). We confirmed these *Nras*^{G12D}copy gains using PCR-MiSeq and also found copy neutral LOH for *Nras*^{G12D} in 3/10 AMLs. In addition, we found copy neutral LOH in 3 of 4 *Npm1*$^{cA/+}$;*Nras*$^{G12D/+}$ AMLs not studied by aCGH. In summary, increased *Nras*^{G12D} dosage was detected

in 11/14 *Npm1*$^{cA/+}$;*Nras*$^{G12D/+}$ AMLs (Figure 4Bii), and this correlated with levels of RAS pathway activation as measured by pERK1/2 staining (Figure 4C).

WES revealed that the average number of single nucleotide variants (SNVs) and small insertions/deletions (indels) per AML sample correlated positively to survival (Figure 5A). *Npm1*$^{cA/+}$ AMLs spontaneously acquired mutations in genes involved in RAS signaling (*Nras*-p.Q61H, *Cbl*-p.S374F, *Ptpn11*-p.S502L, *Nf1*-p.W1260* and *Nf1*-R683*) confirming this genetic interaction. Likewise, we detected a spontaneous tyrosine kinase domain mutation in *Flt3*, (*Flt3*-p.D842G) confirming the importance of FLT3 mutations in progression of NPM1-mutant AML (Figure 5B-C, Supplemental Table 9). Interestingly, a single *Npm1*$^{cA/+}$;*Nras*$^{G12D/+}$ AML harbored an *Idh1*-p.R132Q mutation and mirroring the R132H/R132C mutations commonly seen in human AML[1] whilst IDH1-R132Q itself was reported in human chondrosarcoma.[25] aCGH also revealed complete or partial gain of a minimally amplified region on chr7 in 7/8 *Npm1*$^{cA/+}$ and 4/9 *Npm1*$^{cA/+}$;*Nras*$^{G12D/+}$ AMLs containing genes implicated in leukemogenesis including *Nup98*, *Wee1* and *Eed*, (Supplemental Figure S5C).[7,26-28] Single copy loss of a region containing the epigenetic modifiers Wt1, Asxl1, Dnmt3a (1/8 *Npm1*$^{cA/+}$) and a focal deletion of Ezh2 (1/9 *Npm1*$^{cA/+}$; *Nras*$^{G12D/+}$) were also detected (Figure 5C and Supplemental Figure S5C).

MLL, _Hox_ genes and their partners are required for the survival of _Npm1_^{cA}-driven AML cells.

To assess their contribution to AML maintenance in *Npm1*$^{cA/+}$;*Nras*$^{G12D/+}$ and *Npm1*^{cA};*Flt3*^{ITD} mice, we employed CRISPR-Cas9 to disrupt selected deregulated genes identified by our pre-leukemic GEP, studies. For this, we bred with *Rosa26-EF1-Cas9* animals[11] to generate *Rosa26*$^{Cas9/+}$;*Npm1*$^{cA/+}$;*Nras*$^{G12D/+}$; and *Rosa26*$^{Cas9/+}$;*Npm1*$^{cA/+}$;*Flt3*$^{ITD/+}$ mice. Competitive co-culture of gRNA transduced and non-transduced BM cells from these mice revealed that *Hoxa10* and to a lesser degree *Hoxa9*, but not *Hoxa7* are required for *Npm1*$^{cA/+}$;*Nras*$^{G12D/+}$ and *Npm1*^{cA};*Flt3*$^{ITD/+}$ AML maintenance (Figure 6B). In contrast, all three *HoxA* genes were required for growth of AMLs generated by retroviral *MLL-AF9* transformation of *Flt3*$^{ITD/+}$ BM cells (Supplementary Figure S7C).[11,29,30] Notably, although *Nkx2-3* overexpression enhanced colony-forming ability of wild type and *Flt3*$^{ITD/+}$ BM (Figure 2C), disruption of endogenous *Nkx2-3* did not significantly affect proliferation of *Npm1*$^{cA/+}$;*Nras*$^{G12D/+}$ or *Npm1*^{cA};*Flt3*$^{ITD/+}$ AMLs *in vitro*. Other genes whose disruption reduced proliferation of *Npm1cA*-driven AMLs included *Mll* (*Kmt2a*) gene, recently shown to be a therapeutic target in this AML type[31], *Hoxa9/10* partners or co-factors including *Meis1*, *Pbx1* and *Pbx3*, the *HOXA9* targets *Bcl2* and *Lmo2*[32-34]. A number of genes with altered expression in mutant pre-leukemic MPP cells, were not required for survival of AML cells *in vitro* (Figure 6C). However, we cannot exclude a potential role for these in leukemia initiation.

We also wanted to investigate potential differences in JAK/STAT vs RAS signaling in our AMLs in a similar way. *FLT3-ITD* leads to constitutive activation of JAK/STAT signaling, driving growth and

transformation of hematopoietic cells[35-37]. In keeping with this, our transcriptome analysis revealed that genes involved in JAK/STAT signaling (*Stat5a, Cish, Socs2*) were differentially expressed in *Npm1*^{cA};*Flt3*^{ITD} but not in *Npm1*^{cA};*Nras*^{G12D} Lin$^-$ progenitors. Nevertheless, CRISPR-targeting of *Jak2* and *Stat5a/b* genes inhibited the growth of both *Npm1*^{cA};*Flt3*$^{ITD/+}$ and *Npm1*$^{cA/+}$;*Nras*$^{G12D/+}$ AML cells (Supplemental Figure S8B). We confirmed by RNA-seq that this was due to activation of a JAK/STAT programme in *Npm1*$^{cA/+}$;*Nras*$^{G12D/+}$ AML cells (Figure S9). In this light we conclude that the cytokines required for culturing primary AML cells in vitro (IL-3, IL-6 and SCF), precludes the assessment of signaling genes in AML growth and proliferation.

Discussion

Whilst the mutational drivers of AML and their patterns of co-occurrence are well understood, the molecular basis for the frequency and prognostic impact of these patterns remain unknown. Of particular clinical relevance are the co-occurrence patterns of mutant *NPM1* mutations, which characterize the most common AML subtype[1,2]. Co-mutation of *NPM1* with *FLT3-ITD* is both significantly more frequent and carries a worse prognosis than co-mutation with *RAS genes*.[1,2] To understand the basis of this observation we investigated the interactions of these mutations in bespoke experimental models (Figure 1A). Analysis of the short-term impact of these mutations on hematopoiesis confirmed that single *Npm1*$^{cA/+}$ mutant mice have normal BM cellularity, WCC and splenic weight.[7] As described before, single *Flt3*$^{ITD/+}$ and *Nras*$^{G12D/+}$ had moderate but significant increases in splenic size, whilst *Nras*$^{G12D/+}$ had raised WCC and BM cellularity.[5,6] Introduction of *Npm1*$^{cA/+}$ into the *Nras*$^{G12D/+}$ background did not alter these parameters significantly, yet the *Npm1*$^{cA/+}$;*Flt3*$^{ITD/+}$ co-mutation led to a dramatic rise in WCC and splenic size(Figure 1B). At the cellular level, the *Npm1*$^{cA/+}$;*Nras*$^{G12D/+}$ combination did not change progenitor and stem cell numbers when compared to *Nras*$^{G12D/+}$ alone. In contrast, when compared to *Flt3*$^{ITD/+}$ mutants, *Npm1*$^{cA/+}$;*Flt3*$^{ITD/+}$ mice displayed reductions in CMP and MEP, and increases in LSK progenitors. Furthermore, *Npm1*$^{cA/+}$;*Flt3*$^{ITD/+}$ mice showed a profound reduction in phenotypic HSCs (Figure 1 C–E).

The differential impact of *Npm1*$^{cA/+}$ *on Flt3*$^{ITD/+}$ versus *Nras*$^{G12D/+}$ was reflected in marked differences in GEPs between double mutant mice. The *Npm1*$^{cA/+}$;*Nras*$^{G12D/+}$ model displayed only minimal differences to single *Nras*$^{G12D/+}$, whilst *Npm1*$^{cA/+}$;*Flt3*$^{ITD/+}$ lin$^-$ progenitors had profoundly different GEPs to *Flt3*$^{ITD/+}$. From these and complimentary analyses of human *NPM1c* AML we identify *NKX2-3* as a marker of this type of AML. Expression of *NKX2-3* distinguishes *MLL-AF6* and *MLL-ENL* from other forms of *MLL*-mutant leukemia[21,38], highlighting the mechanistic links between *NPM1c*- and *MLL*-fusion genes. Here, we show that whilst potent overexpression of *Nkx2.3* by lentivirus may have

an impact on self-renewal, genetic disruption of the endogenous *Nkx2.3* did not inhibit AML cell growth (Figure 6).

We went on to age double mutant mice and report that, like *Npm1*$^{cA/+}$;*Flt3*$^{ITD/+}$ animals, *Npm1*$^{cA/+}$;*Nras*$^{G12D/+}$ mice also develop highly penetrant AML, albeit with a much longer latency and a more mature phenotype overall. Interestingly single mutant *Flt3*$^{ITD/+}$ and *Nras*$^{G12D/+}$ mice had similar survival (Figure 3A), indicating that the interaction with *Npm1*^{cA} was central to this difference. To understand the genetic events involved in leukemic progression, we performed exome sequencing and copy number analysis of *Npm1*$^{cA/+}$;*Flt3*$^{ITD/+}$ and *Npm1*$^{cA/+}$;*Nras*$^{G12D/+}$ AMLs. Interestingly, the commonest somatic event during AML progression was an increase in *Nras*$^{G12D/+}$ or *Flt3*$^{ITD/+}$ mutant allele burden, through copy-neutral LOH or copy number gain. In human AML, copy-neutral LOH is common for *FLT3-ITD*, but less so for mutant *NRAS*; for example in a recent study we identified only one such LOH event amongst 13 *RAS* mutant human AMLs.[13] Nevertheless, in keeping with our findings, studies using the *Nras*$^{G12D/+}$ model, in combination with retroviral insertional mutagenesis, resulted in high penetrance AML with frequent LOH for *Nras-G12D* when combined with overexpression of oncogenes such as *Evi1*.[6,39] The different incidence of LOH for mutant *RAS* between murine and human AML may operate through the fact that, compared to the acquisition of other oncogenic mutations (e.g. *Idh1*-R132Q in our study), LOH for *Nras-G12D* may be more expedient in mice given the large numbers of *Npm1*$^{cA/+}$/*Nras*$^{G12D/+}$ pre-leukemic HSCs. Other possible reasons may relate to the differences in human-mouse synteny and the fact that mice are inbred potentially making recombination events more likely. Notwithstanding mouse-human differences in LOH frequencies, our data provide strong evidence that increased mutant *Flt3* and *Ras* gene dosage are important for leukemic transformation/progression.

Finally, in order to investigate their role in *Npm1c* AML, we use CRISPR-Cas9 to disrupt selected genes in Cas9-expressing primary mouse leukemia cells. Using this approach we confirmed the requirement for the HoxA9/10 functional gene network in *Npm1c* AML maintenance. Interestingly, although it is widely appreciated that overexpression of *Hoxa9* stimulates leukemic transformation [22,29,33], in our model disruption of *Hoxa10* has a more detrimental impact on survival, mirroring our recent genome wide essentiality screen in the NPM1c-harboring OCI-AML3 cell line.[11]

Our study describes the first faithful mouse model of the interaction of Npm1c with *Nras*-G12D, the preferred form of oncogenic NRAS in human AML.[2] Both NPM1c models share a number of salient characteristics, which are imparted by mutant Npm1, such as homeobox gene overexpression and increased self-renewal of hemopoietic progenitors. However, we demonstrate that the co-occurrence of *Npm1c/Flt3-ITD* is significantly more leukemogenic and leads to strikingly different

molecular and cellular consequences compared to *Npm1c/Nras-G12D*, providing a mechanistic explanation for the higher frequency and worse prognosis of NPM1c/ FLT3-ITD AML. Furthermore, through the generation of Cas9-expressing AML models, we also present a versatile approach for the study of genetic interactions in primary mouse leukemias using CRISPR. Whilst our non-Cas9-expressing *Npm1c/Flt3-ITD* model was helpful in recent studies of new anti-AML therapies[31], these Cas9-expressing models can be utilized to study both genetic and pharmacological interactions in parallel, and also to perform targeted mechanistic studies.

[3966 words]

Acknowledgements

We thank Professor Gary Gilliland for the *Flt3*^{ITD} mouse and Professors Kevin Shannon and Tyler Jacks for the *Nras*^{G12D} mouse. We would also like to thank Mark Dawson for the kind gift of the *MLL-AF9* retroviral construct. OMD, JLC and GSV are funded by a Wellcome Trust Senior Fellowship in Clinical Science (WT095663MA). AM was funded by the Kay Kendall Leukaemia Fund project grant (KKL634). CG was funded by a Bloodwise Clinical Research Training Fellowship. IV is funded by Spanish Ministerio de Economía y Competitividad subprograma Ramón y Cajal. We thank Servicio Santander Supercomputación for their support. GSV is a consultant for and holds stock in Kymab Ltd, and receives an educational grant from Celgene.

Authorship

Contribution: O.M.D., J.L.C., A.M., C.S.G., C.L., P.G. and G.S.V. performed mouse experiments. O.M.D. and G.S.V. analyzed results; P.W. and M.A. performed histopathological analysis of mouse samples; O.M.D., N.C., R.M.A. and MS. V. performed transcriptome analysis; I.V. performed analysis of next generation sequencing; O.M.D, S.P. and K.T. performed CRIPSR-CAS9 experiments; O.M.D. and G.S.V. designed the study. O.M.D. and G.S.V. wrote the paper with the help of R.R., P.W., M.A. and A.B.

Conflict of interest disclosure: GSV is a consultant for and holds stock in Kymab Ltd, and receives an educational grant from Celgene. All other authors declare no competing financial interests.

Correspondence: George Vassiliou, [1]The Wellcome Trust Sanger Institute, Wellcome Trust Genome Campus, Hinxton, Cambridge, CB10 1SA, UK; e-mail: gsv20@sanger.ac.uk.

418
419
420
421

422

423 **Figure Legends**

424 **Figure 1. Mutant *Npm1* co-operates with *Nras*-G12D and *Flt3*-ITD to enhance myeloid**
425 **differentiation and enhance progenitor self-renewal.**

426 (**A**) Schema for *Mx-1 Cre*, $Npm1^{flox\text{-}cA}$, $Nras^{LSL\text{-}G12D}$ and $Flt3^{ITD}$ inter-crosses. (**B**) $Nras^{G12D/+}$ mice show a
427 subtle and $Npm1^{cA/+}$; $Flt3^{ITD/+}$ mice a marked increase in white cell count (WCC), compared to
428 wildtype. Splenic sizes were significantly increased in all mutant genotypes except $Npm1^{cA/+}$, with
429 $Npm1^{cA/+}$; $Flt3^{ITD/+}$ showing the most striking phenotype. Bone marrow cellularity was increased only
430 in the presence of the $Nras^{G12D/+}$ allele. (**C**) FACS analysis at 4-5 weeks after mutation induction.
431 Gating strategies depicted are from wildtype mice. Significant differences in the stem and progenitor
432 cell compartments of $Nras^{G12D/+}$ and $Flt3^{ITD/+,}$ but not $Npm1^{cA/+}$ single mutant mice, as previously
433 reported. In double mutant mice, the $Npm1^{cA/+}$; $Nras^{G12D/+}$ combination was not significantly
434 different to $Nras^{G12D/+}$, in contrast to $Npm1^{cA/+}$;$Flt3^{ITD/+}$ which was markedly different to both $Flt3^{ITD/+}$
435 *and* $Npm1^{cA/+}$ single mutants. (**D**) Using a cell surface phenotype independent of FLT3 staining, we
436 found that CD45+/EPCR+/CD150+/CD48- HSCs were reduced slightly in $Npm1^{cA/+}$;$Nras^{G12D/+}$ and
437 markedly in $Npm1^{cA/+}$;$Flt3^{ITD/+}$mice. (**E**) Summary of hematopoietic effects of $Npm1^{cA/+}$;$Nras^{G12D/+}$ and
438 $Npm1^{cA/+}$;$Flt3^{ITD/+}$ double mutations in mice. LK, Lin^-/Kit^+; LSK, $Lin^-/Sca\text{-}1^+/Kit^+$; CMP, common myeloid
439 progenitor; MEP, megakaryocyte-erythroid progenitor; GMP, granulocyte-monocyte progenitor;
440 MPP, multi-potent progenitor; LMPP, lymphoid primed multi-potent progenitor; CLP, common
441 lymphoid progenitor and HSC, hematopoietic stem cell. (**F**) Single $Npm1^{cA/+}$ and double
442 $Npm1^{cA/+}$;$Nras^{G12D/+}$ or $Npm1^{cA/+}$;$Flt3^{ITD/+}$ mutant hematopoietic progenitors show increased self-
443 renewal potential in whole bone marrow serial replating assays (n=4-8). Mean ±SEM are plotted.
444 Significant values are reported for one-way analysis of variance (ANOVA, Bonferroni adjusted); (*
445 P<0.05 vs wildtype, ** P<0.01 vs wildtype, *** P<0.001 vs wildtype), (Δ P<0.05 vs $Flt3^{ITD/+}$,
446 ΔΔ P<0.01 vs $Flt3^{ITD/+}$, ΔΔΔ P<0.001 vs $Flt3^{ITD/+}$), (♣ P<0.05 vs $Nras^{G12D/+}$, ♣♣ P<0.01 vs $Nras^{G12D/+}$,
447 ♣♣♣ P<0.001 vs $Nras^{G12D/+}$), († P<0.05 $Npm1^{cA/+}$; $Nras^{G12D/+}$ vs $Npm1^{cA/+}$; $Flt3^{ITD/+}$, †† P<0.01 $Npm1^{cA/+}$;
448 $Nras^{G12D/+}$ vs $Npm1^{cA/+}$; $Flt3^{ITD/+}$, ††† P<0.001 $Npm1^{cA/+}$; $Nras^{G12D/+}$ vs $Npm1^{cA/+}$; $Flt3^{ITD/+}$).

449 **Figure 2. Impact of $Npm1^{cA/+}$ on the transcriptome of $Nras^{G12D/+}$ and $Flt3^{ITD/+}$ mutant hematopoietic**
450 **progenitors.**

451 (**A**) Overlap of differentially expressed mRNAs reveals that $Npm1^{cA/+}$ has a dramatic impact on Lin-
452 progenitor GEPs when combined with $Flt3^{ITD/+}$, but only a modest impact when combined with
453 $Nras^{G12D/+}$. Nonetheless, the characteristic hallmarks of $Npm1^{cA/+}$ are retained in both double mutant
454 progenitors, namely overexpression of *Hoxa* genes and of the homeobox genes *Hopx* and *Nkx2-3*
455 (also seen in single $Npm1^{cA/+}$ progenitors). Gene Set Enrichment Analysis reveals enrichment of

differentially expressed genes from these models in human AMLs harboring mutant *NPM1* or *MLL* gene fusions (**B**) Comparison of human *NPM1*-mutant (*NPM1*^{c}) versus *NPM1-wildtype (NPM1*^{WT}) normal karyotype AML (NK-AML) also shows marked overexpression of *HOXA* and *HOXB* genes, as well as of *NKX2.3* raising the possibility that the latter may mediate some of the effect of *NPM1*^{c}. (**C**) Effects of *Nkx2-3* and *Hoxa9* over-expression on mouse hematopoietic progenitors. (i) Lin^{-} bone marrow progenitors from wildtype *and Flt3*$^{ITD/+}$ mice were transduced with MSCV-*Nkx2.3*-CFP and/or MSCV-*Hoxa9*-GFP constructs, maintained in liquid culture for 7 days, FACS sorted for CFP and GFP single and for double transfected cells and plated in semi-solid media. (ii) Colony assays of 2,500 transduced cells show that both MSCV-*Hoxa9* and MSCV-*Nkx2-3* conferred an increase in self-renewal of both wildtype and *Flt3*$^{ITD/+}$ cells. However, double MSCV-*Hoxa9*/MSCV-*Nkx2-3* transfected cells showed no further changes in self-renewal when compared to MSCV-*Hoxa9* alone. Mean ± SEM (n=3); *p<0.05; **p<0.01; ***p<0.001; students t-test). (**D**) Sorting strategy for LSK/CD34^{+}/Flt3^{+}/CD48^{+} progenitor cells and overlap of differentially expressed genes (Illumina MouseWG-6 v2 Expression BeadChip) for (i) *Nras*$^{G12D/+}$ vs *Npm1*$^{cA/+}$*;Nras*$^{G12D/+}$ and (ii) *Flt3*$^{ITD/+}$ vs *Npm1*$^{cA/+}$*;Flt3*$^{ITD/+}$ MPPs datasets. (**E**) Heat map of normalised *Hox* gene expression in purified (i) MPP and (ii) Lin^{-} populations reveal that *Npm1*$^{cA/+}$ mutants (single or double) have similar patterns of *Hox* gene expression to wildtype (normalised average expression values are used to generate heat map values). (**F**) Differentially expressed genes in *Npm1*$^{cA/+}$*;Flt3*$^{ITD/+}$ MPPs vs wildtype controls .

Figure 3. *Npm1*^{cA} and *Nras*^{G12D} co-operate to drive high penetrance AML.

(**A**) Kaplan Meier survival curves of wildtype (n=23), *Npm1*$^{cA/+}$ (n=34), *Nras*$^{G12D/+}$ (n=40), *Flt3*$^{ITD/+}$ (n=39), *Npm1*$^{cA/+}$*;Nras*$^{G12D/+}$ (n=46) and *Npm1*$^{cA/+}$*;Flt3*$^{ITD+/}$ (n=40). Double mutant (*Npm1*$^{cA/+}$*;Nras*$^{G12D/+}$ and *Npm1*$^{cA/+}$*;Flt3*$^{ITD/+}$) mice had a significantly shortened survival when compared to single mutants, whilst *Npm1*$^{cA/+}$*;Flt3*^{ITD} had significantly shorter survival than *Npm1*$^{cA/+}$*;Nras*$^{G12D/+}$ mice. (**B**) Results of independent histopathological analysis of aged moribund mice. Incidence of AML in compound *Npm1*$^{cA/+}$*;Nras*$^{G12D/+}$ and *Npm1*$^{cA/+}$*;Flt3*$^{ITD/+}$ mice is increased compared to *Npm1*$^{cA/+}$, *Nras*$^{G12D/+}$ and *Flt3*$^{ITD/+}$ mice. Examples of complete effacement of splenic tissue and infiltration of myeloid blast cells in liver tissue from *Npm1*$^{cA/+}$*; Nras*$^{G12D/+}$ and *Npm1*$^{cA/+}$*; Flt3*$^{ITD+/}$ AMLs are presented. Reduced MPO staining in diseased tissues is observed in samples categorized as AML without maturation (AML-) compared to those categorized as AML with maturation (AML+). H&E, Haematoxylin and eosin; MPO, myeloperoxidase.

Figure 4. Leukemic progression in double mutant mice involves increased *Nras*^{G12D} or *Flt3*^{ITD} allele dosage

(**A)** Increase in *Flt3*^{ITD} allele burden in AMLs from *Npm1*^{cA}*; Flt3*^{ITD} mice through loss of heterozygosity for the locus. (i) *Flt3*^{ITD} amplicon sequencing (MiSeq) of leukemic bone marrow or spleen DNA (FN2-FN7). Tail DNA amplified from 2-week-old Flt3$^{+/+}$, *Flt3*$^{ITD/+}$, *Flt3*$^{ITD/ITD}$ mice was used as control. (ii) Normalised Log2 ratio plots show copy neutrality of chr5 and the Flt3 locus in 7/7 *Npm1*^{cA}*; Flt3*^{ITD} murine AMLs (FN-AMLs) tested. (**B)** (i) Summary of aCGH showing copy number gain at the *Nras* locus in AMLs RN6-10. (ii) Allele fractions for *Nras*^{wt} vs *Nras*^{G12D} show that copy number gains in RN6-

10 involved $Nras^{G12D}$, and that an additional 3 cases (RN3-5) show copy-neutral loss-of-heterozygosity. In addition, two more RN AMLs show gains in mutant NRAS when measuring $Nras^{wt}$ vs $Nras^{G12D}$ allele fractions (aCGH was not performed on these). Results of two $Npm1^{cA/+}$ samples are also shown for comparison purposes (N6, N7). (**C**) Increased gene dosage of $Nras^{G12D}$ correlates with increased levels of phosphorylated RAS effectors pERK1/2. FN2,3,4,6,7= $Npm1^{cA}$;$Flt3^{ITD}$ AML, RN1-14= $Npm1^{cA/+}$;$Nras^{G12D/+}$ AML.

Figure 5. Somatic mutations in $Npm1^{cA/+}$, $Npm1^{cA/+}$; $Nras^{G12D/+}$ and $Npm1^{cA}$; $Flt3^{ITD}$AMLs. (**A**) Exome sequencing identifies an increased number of somatic nucleotide variants (SNVs) and small indels in $Npm1^{cA/+}$, compared to $Npm1^{cA/+}$; $Nras^{G12D/+}$ (RN-AML) and $Npm1^{cA}$; $Flt3^{ITD}$ (FN-AML) AML samples. $Npm1^{cA/+}$ 6.8±0.9, $Npm1^{cA/+}$; $Nras^{G12D/+}$ 3.3±0.5 and $Npm1^{cA/+}$; $Flt3^{ITD/+}$2.6±0.7 (mean±SEM) (** $p<0.01$ vs $Npm1^{cA/+}$ one way ANOVA, Bonferroni adjusted). Total AMLs sequenced; $Npm1^{cA/+}$ (n=12), $Npm1^{cA/+}$; $Nras^{G12D/+}$ (n=14) and $Npm1^{cA}$; $Flt3^{ITD}$ (n=7). (**B**) Summary of SNVs/Indels detected in AMLs from each genotype as indicated. Those in blue are genes mutated in the TCGA AML dataset. Those in red are exact or synonymous mutations detected in the TCGA AML dataset. (**C**) Co-occurrence of SNVs and CNVs. Depicted are SNVs and focal copy number variations (CNVs) which have been formally detected in the TCGA AML[19] dataset or detected as common insertion sites (CIS) in our previously published $Npm1^{cA/+}$ Sleeping Beauty Transposon screen [18] . Mutant allele copy gains, chromosome gains and losses depicted. For copy number variation, colour coded boxes are based on log2 ratios (aCGH) and are not representative of CNV size. For a complete overview of all CNV and SNV co-occurrence see Supplemental Figure S6.

Figure 6. *MLL*, *Hox* genes and their partners are required for the survival of $Npm1^{cA}$-driven AML cells. (**A**) Schematic depicting the derivation and liquid culture of *Rosa26-EF1-Cas9* expressing AML cell lines. CRISPR-EF1-Cas9 based assessment of individual genes aberrantly expressed in $Npm1^{cA/+}$;$Nras^{G12D/+}$ and $Npm1^{cA}$;$Flt3^{ITD}$ mice. CAS9 activity of these mouse AML cell lines was validated as described previously (Supplementary Figure S7A).[11] Individual *Rosa26-EF1-Cas9* expressing cell lines were derived from two mice of each genotype. *In vitro* competitive assays were performed over a 23 day period using AML cell lines transduced with lentivirus expressing gRNAs for the indicated gene, and the BFP-positive fraction compared with the non-transduced population. Results were normalized to day 3 for each gRNA. Results from AML cell lines transduced with guide RNAs targeting Hoxa-related (**B**) and non-Hoxa related (**C**) genes. gRNA sequences were selected from a previously published library[11] and are detailed in Supplementary Table S15. Guides against the pan essential Npm1 gene are used as a control.

References

1. Cancer Genome Atlas Research N, Ley TJ, Miller C, et al. Genomic and epigenomic landscapes of adult de novo acute myeloid leukemia. *N Engl J Med.* 2013;368(22):2059-2074.
2. Papaemmanuil E, Gerstung M, Bullinger L, et al. Genomic Classification and Prognosis in Acute Myeloid Leukemia. *N Engl J Med.* 2016;374(23):2209-2221.
3. Falini B, Mecucci C, Tiacci E, et al. Cytoplasmic nucleophosmin in acute myelogenous leukemia with a normal karyotype. *N Engl J Med.* 2005;352(3):254-266.
4. Welch JS, Ley TJ, Link DC, et al. The origin and evolution of mutations in acute myeloid leukemia. *Cell.* 2012;150(2):264-278.
5. Lee BH, Tothova Z, Levine RL, et al. FLT3 mutations confer enhanced proliferation and survival properties to multipotent progenitors in a murine model of chronic myelomonocytic leukemia. *Cancer Cell.* 2007;12(4):367-380.
6. Li Q, Haigis KM, McDaniel A, et al. Hematopoiesis and leukemogenesis in mice expressing oncogenic NrasG12D from the endogenous locus. *Blood.* 2011;117(6):2022-2032.
7. Vassiliou GS, Cooper JL, Rad R, et al. Mutant nucleophosmin and cooperating pathways drive leukemia initiation and progression in mice. *Nat Genet.* 2011;43(5):470-475.
8. Mupo A, Celani L, Dovey O, et al. A powerful molecular synergy between mutant Nucleophosmin and Flt3-ITD drives acute myeloid leukemia in mice. *Leukemia.* 2013;27(9):1917-1920.
9. Mallardo M, Caronno A, Pruneri G, et al. NPMc+ and FLT3_ITD mutations cooperate in inducing acute leukaemia in a novel mouse model. *Leukemia.* 2013;27(11):2248-2251.
10. Sportoletti P, Varasano E, Rossi R, et al. Mouse models of NPM1-mutated acute myeloid leukemia: biological and clinical implications. *Leukemia.* 2015;29(2):269-278.
11. Tzelepis K, Koike-Yusa H, De Braekeleer E, et al. A CRISPR Dropout Screen Identifies Genetic Vulnerabilities and Therapeutic Targets in Acute Myeloid Leukemia. *Cell Rep.* 2016;17(4):1193-1205.
12. McKerrell T, Park N, Moreno T, et al. Leukemia-associated somatic mutations drive distinct patterns of age-related clonal hemopoiesis. *Cell Rep.* 2015;10(8):1239-1245.
13. McKerrell T, Moreno T, Ponstingl H, et al. Development and validation of a comprehensive genomic diagnostic tool for myeloid malignancies. *Blood.* 2016;128(1):e1-9.
14. Li Q, Bohin N, Wen T, et al. Oncogenic Nras has bimodal effects on stem cells that sustainably increase competitiveness. *Nature.* 2013;504(7478):143-147.
15. Wang J, Kong G, Liu Y, et al. Nras(G12D/+) promotes leukemogenesis by aberrantly regulating hematopoietic stem cell functions. *Blood.* 2013;121(26):5203-5207.
16. Mead AJ, Kharazi S, Atkinson D, et al. FLT3-ITDs instruct a myeloid differentiation and transformation bias in lymphomyeloid multipotent progenitors. *Cell Rep.* 2013;3(6):1766-1776.
17. Shih AH, Jiang Y, Meydan C, et al. Mutational cooperativity linked to combinatorial epigenetic gain of function in acute myeloid leukemia. *Cancer Cell.* 2015;27(4):502-515.
18. Akashi K, Traver D, Miyamoto T, Weissman IL. A clonogenic common myeloid progenitor that gives rise to all myeloid lineages. *Nature.* 2000;404(6774):193-197.
19. Kent DG, Copley MR, Benz C, et al. Prospective isolation and molecular characterization of hematopoietic stem cells with durable self-renewal potential. *Blood.* 2009;113(25):6342-6350.
20. Spencer DH, Young MA, Lamprecht TL, et al. Epigenomic analysis of the HOX gene loci reveals mechanisms that may control canonical expression patterns in AML and normal hematopoietic cells. *Leukemia.* 2015;29(6):1279-1289.
21. Lavallee VP, Baccelli I, Krosl J, et al. The transcriptomic landscape and directed chemical interrogation of MLL-rearranged acute myeloid leukemias. *Nat Genet.* 2015;47(9):1030-1037.

22. Thorsteinsdottir U, Mamo A, Kroon E, et al. Overexpression of the myeloid leukemia-associated Hoxa9 gene in bone marrow cells induces stem cell expansion. *Blood.* 2002;99(1):121-129.
23. Kogan SC, Ward JM, Anver MR, et al. Bethesda proposals for classification of nonlymphoid hematopoietic neoplasms in mice. *Blood.* 2002;100(1):238-245.
24. Stirewalt DL, Pogosova-Agadjanyan EL, Tsuchiya K, Joaquin J, Meshinchi S. Copy-neutral loss of heterozygosity is prevalent and a late event in the pathogenesis of FLT3/ITD AML. *Blood Cancer J.* 2014;4:e208.
25. Hirata M, Sasaki M, Cairns RA, et al. Mutant IDH is sufficient to initiate enchondromatosis in mice. *Proc Natl Acad Sci U S A.* 2015;112(9):2829-2834.
26. Weisberg E, Nonami A, Chen Z, et al. Identification of Wee1 as a novel therapeutic target for mutant RAS-driven acute leukemia and other malignancies. *Leukemia.* 2015;29(1):27-37.
27. Shi J, Wang E, Zuber J, et al. The Polycomb complex PRC2 supports aberrant self-renewal in a mouse model of MLL-AF9;Nras(G12D) acute myeloid leukemia. *Oncogene.* 2013;32(7):930-938.
28. Danis E, Yamauchi T, Echanique K, et al. Inactivation of Eed impedes MLL-AF9-mediated leukemogenesis through Cdkn2a-dependent and Cdkn2a-independent mechanisms in a murine model. *Exp Hematol.* 2015;43(11):930-935 e936.
29. Kumar AR, Hudson WA, Chen W, Nishiuchi R, Yao Q, Kersey JH. Hoxa9 influences the phenotype but not the incidence of Mll-AF9 fusion gene leukemia. *Blood.* 2004;103(5):1823-1828.
30. Dawson MA, Prinjha RK, Dittmann A, et al. Inhibition of BET recruitment to chromatin as an effective treatment for MLL-fusion leukaemia. *Nature.* 2011;478(7370):529-533.
31. Kuhn MW, Song E, Feng Z, et al. Targeting Chromatin Regulators Inhibits Leukemogenic Gene Expression in NPM1 Mutant Leukemia. *Cancer Discov.* 2016;6(10):1166-1181.
32. Brumatti G, Salmanidis M, Kok CH, et al. HoxA9 regulated Bcl-2 expression mediates survival of myeloid progenitors and the severity of HoxA9-dependent leukemia. *Oncotarget.* 2013;4(11):1933-1947.
33. Collins CT, Hess JL. Role of HOXA9 in leukemia: dysregulation, cofactors and essential targets. *Oncogene.* 2016;35(9):1090-1098.
34. Huang Y, Sitwala K, Bronstein J, et al. Identification and characterization of Hoxa9 binding sites in hematopoietic cells. *Blood.* 2012;119(2):388-398.
35. Dovey OM, Chen B, Mupo A, et al. Identification of a germline F692L drug resistance variant in cis with Flt3-internal tandem duplication in knock-in mice. *Haematologica.* 2016;101(8):e328-331.
36. Choudhary C, Brandts C, Schwable J, et al. Activation mechanisms of STAT5 by oncogenic Flt3-ITD. *Blood.* 2007;110(1):370-374.
37. Chatterjee A, Ghosh J, Ramdas B, et al. Regulation of Stat5 by FAK and PAK1 in Oncogenic FLT3- and KIT-Driven Leukemogenesis. *Cell Rep.* 2014;9(4):1333-1348.
38. Garcia-Cuellar MP, Buttner C, Bartenhagen C, Dugas M, Slany RK. Leukemogenic MLL-ENL Fusions Induce Alternative Chromatin States to Drive a Functionally Dichotomous Group of Target Genes. *Cell Rep.* 2016;15(2):310-322.
39. Xu J, Haigis KM, Firestone AJ, et al. Dominant role of oncogene dosage and absence of tumor suppressor activity in Nras-driven hematopoietic transformation. *Cancer Discov.* 2013;3(9):993-1001.

Figure 1.

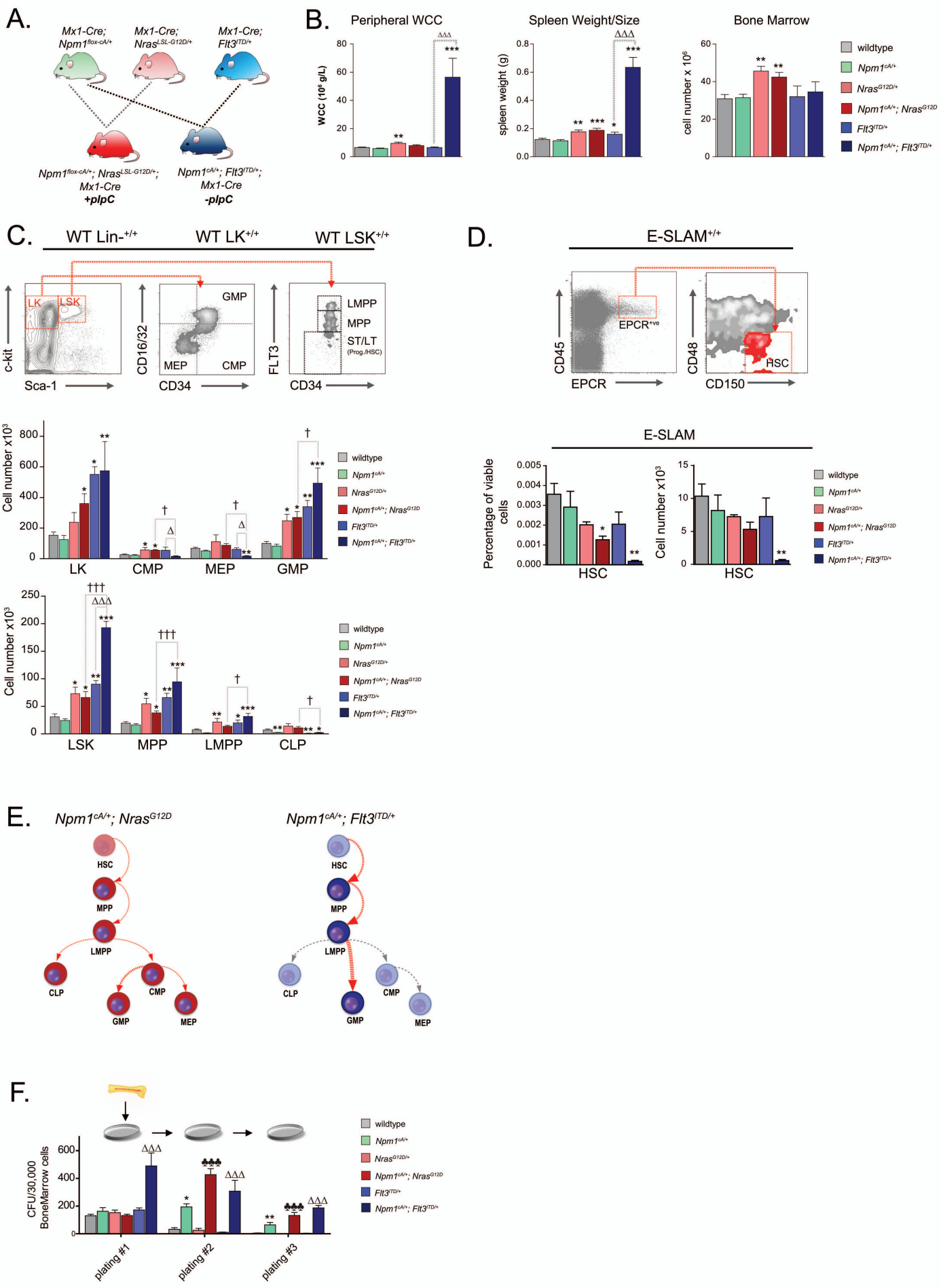
A.
Mx1-Cre; Npm1flox-cA/+
Mx1-Cre; NrasLSL-G12D/+
Mx1-Cre; Flt3ITD/+
Npm1flox-cA/+; NrasLSL-G12D/+; Mx1-Cre +plpC
Npm1cA/+; Flt3ITD/+; Mx1-Cre -plpC
B.
Peripheral WCC
WCC (10⁹ g/L)
Spleen Weight/Size
spleen weight (g)
Bone Marrow
cell number x 10⁶
wildtype
Npm1cA/+
NrasG12D/+
Npm1cA/+; NrasG12D
Flt3ITD/+
Npm1cA/+; Flt3ITD/+
C.
WT Lin-+/+
WT LK+/+
WT LSK+/+
c-kit
Sca-1
LK
LSK
CD16/32
CD34
GMP
MEP
CMP
FLT3
LMPP
MPP
ST/LT (Prog./HSC)
Cell number x10³
LK
CMP
MEP
GMP
LSK
MPP
LMPP
CLP
D.
E-SLAM+/+
CD45
EPCR
EPCR+ve
CD48
CD150
HSC
E-SLAM
Percentage of viable cells
Cell number x10³
E.
Npm1cA/+; NrasG12D
Npm1cA/+; Flt3ITD/+
HSC
MPP
LMPP
CLP
CMP
GMP
MEP
F.
CFU/30,000 BoneMarrow cells
plating #1
plating #2
plating #3

Figure 2

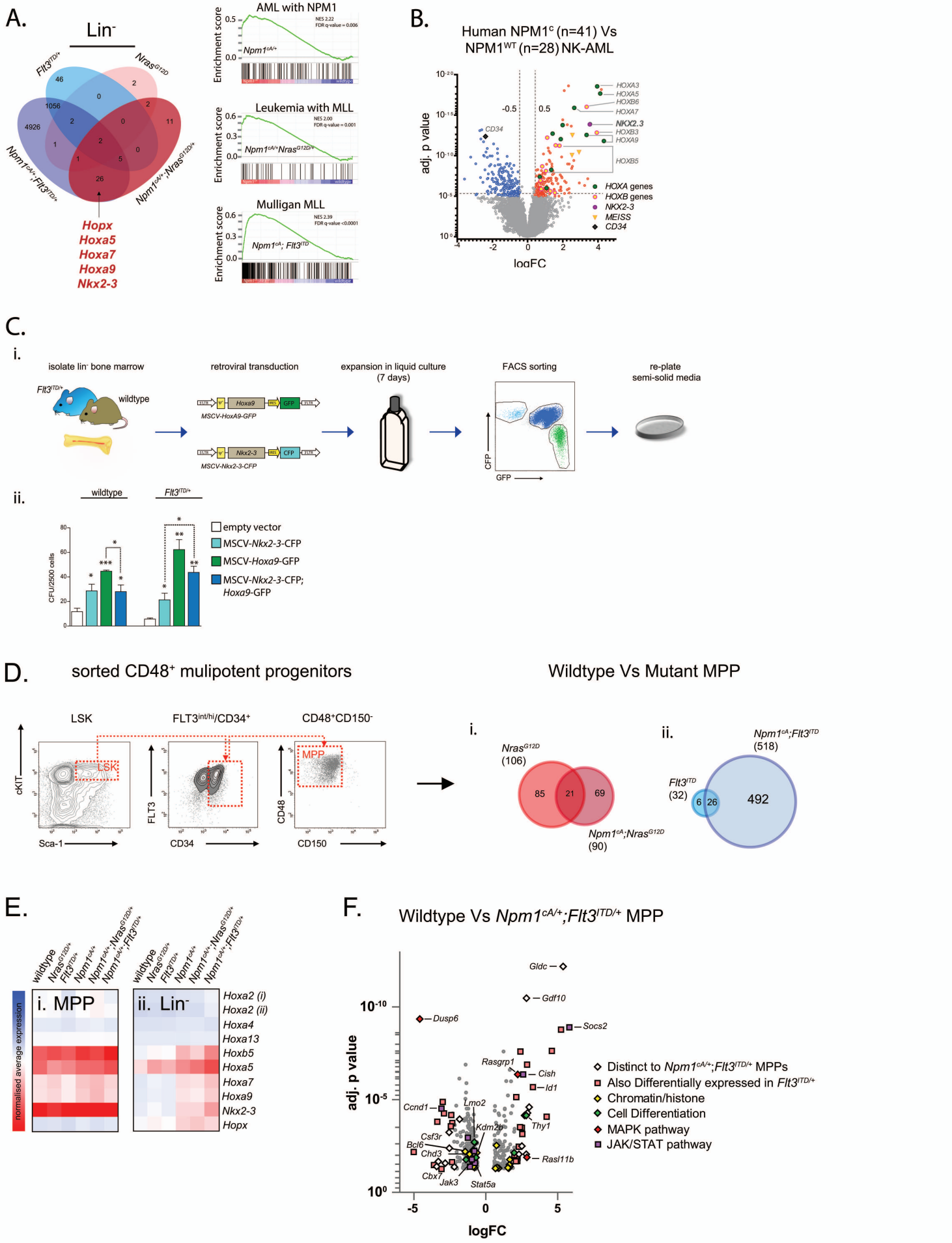
A.
Lin-
Flt3ITD/+
NrasG12D
Npm1cA/+;Flt3ITD/+
Npm1cA/+;NrasG12D/+
Hopx
Hoxa5
Hoxa7
Hoxa9
Nkx2-3
AML with NPM1
Leukemia with MLL
Mulligan MLL
Enrichment score
B.
Human NPM1c (n=41) Vs
NPM1WT (n=28) NK-AML
adj. p value
logFC
HOXA genes
HOXB genes
NKX2-3
MEISS
CD34
C.
i.
isolate lin- bone marrow
retroviral transduction
expansion in liquid culture
(7 days)
FACS sorting
re-plate
semi-solid media
wildtype
MSCV-HoxA9-GFP
MSCV-Nkx2-3-CFP
ii.
CFU/2500 cells
empty vector
MSCV-Nkx2-3-CFP
MSCV-Hoxa9-GFP
MSCV-Nkx2-3-CFP;
Hoxa9-GFP
D.
sorted CD48+ mulipotent progenitors
Wildtype Vs Mutant MPP
LSK
FLT3int/hi/CD34+
CD48+CD150-
cKIT
Sca-1
FLT3
CD34
CD48
CD150
MPP
NrasG12D
(106)
Npm1cA;NrasG12D
(90)
Npm1cA;Flt3ITD
(518)
Flt3ITD
(32)
492
E.
wildtype
NrasG12D/+
Flt3ITD/+
Npm1cA/+
Npm1cA/+;NrasG12D/+
Npm1cA/+;Flt3ITD/+
i. MPP
ii. Lin-
normalised average expression
Hoxa2 (i)
Hoxa2 (ii)
Hoxa4
Hoxa13
Hoxb5
Hoxa5
Hoxa7
Hoxa9
Nkx2-3
Hopx
F.
Wildtype Vs Npm1cA/+;Flt3ITD/+ MPP
adj. p value
logFC
Distinct to Npm1cA/+;Flt3ITD/+ MPPs
Also Differentially expressed in Flt3ITD/+
Chromatin/histone
Cell Differentiation
MAPK pathway
JAK/STAT pathway

Figure 3

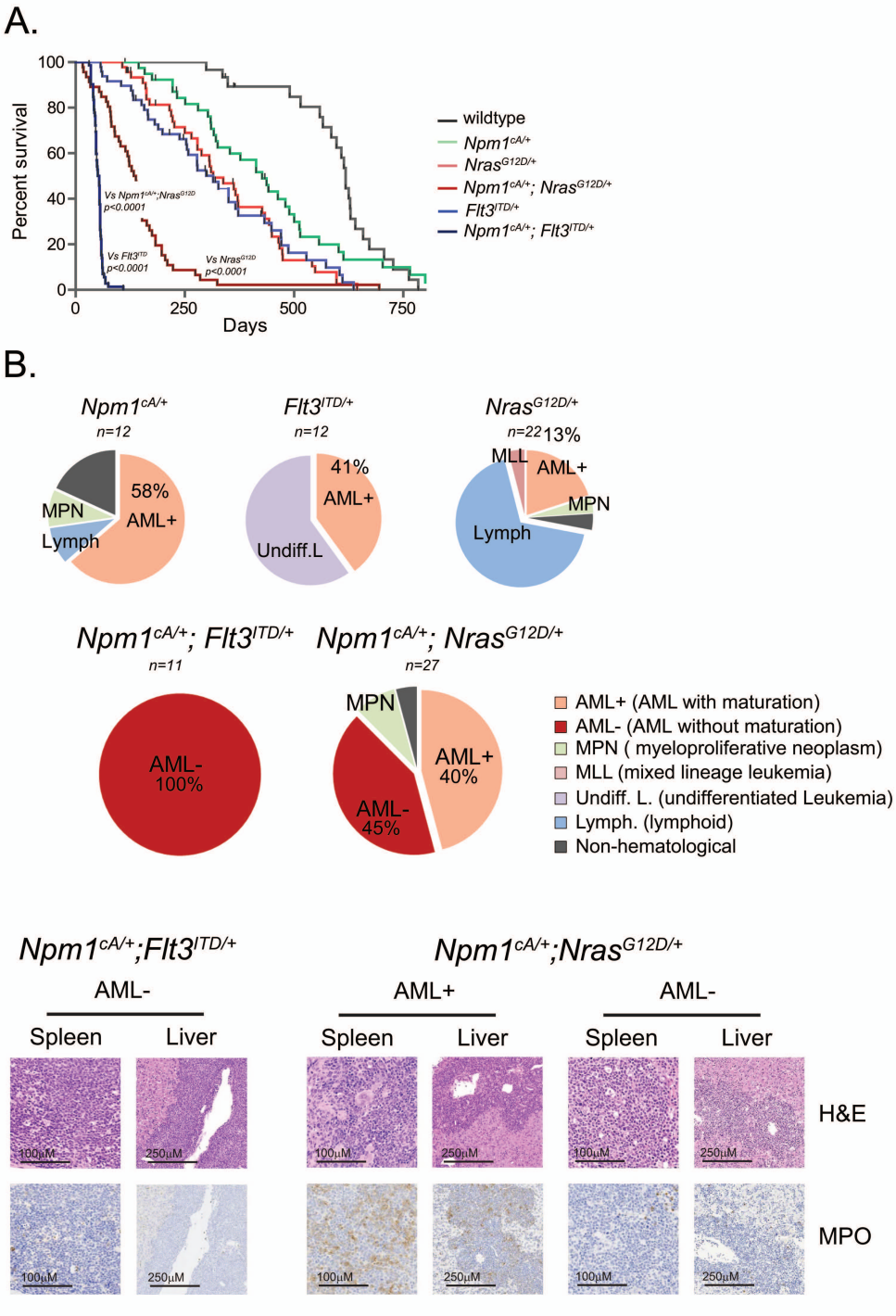
A.
Percent survival
Days
Vs Npm1cA/+;NrasG12D p<0.0001
Vs Flt3ITD p<0.0001
Vs NrasG12D p<0.0001
wildtype
Npm1cA/+
NrasG12D/+
Npm1cA/+; NrasG12D/+
Flt3ITD/+
Npm1cA/+; Flt3ITD/+
B.
Npm1cA/+ n=12
58% AML+
MPN
Lymph
Flt3ITD/+ n=12
41% AML+
Undiff.L
NrasG12D/+ n=22
13% MLL
AML+
MPN
Lymph
Npm1cA/+; Flt3ITD/+ n=11
AML- 100%
Npm1cA/+; NrasG12D/+ n=27
MPN
AML+ 40%
AML- 45%
AML+ (AML with maturation)
AML- (AML without maturation)
MPN (myeloproliferative neoplasm)
MLL (mixed lineage leukemia)
Undiff. L. (undifferentiated Leukemia)
Lymph. (lymphoid)
Non-hematological
Npm1cA/+;Flt3ITD/+
AML-
Spleen
Liver
Npm1cA/+;NrasG12D/+
AML+
AML-
H&E
MPO
100μM
250μM

Figure 4

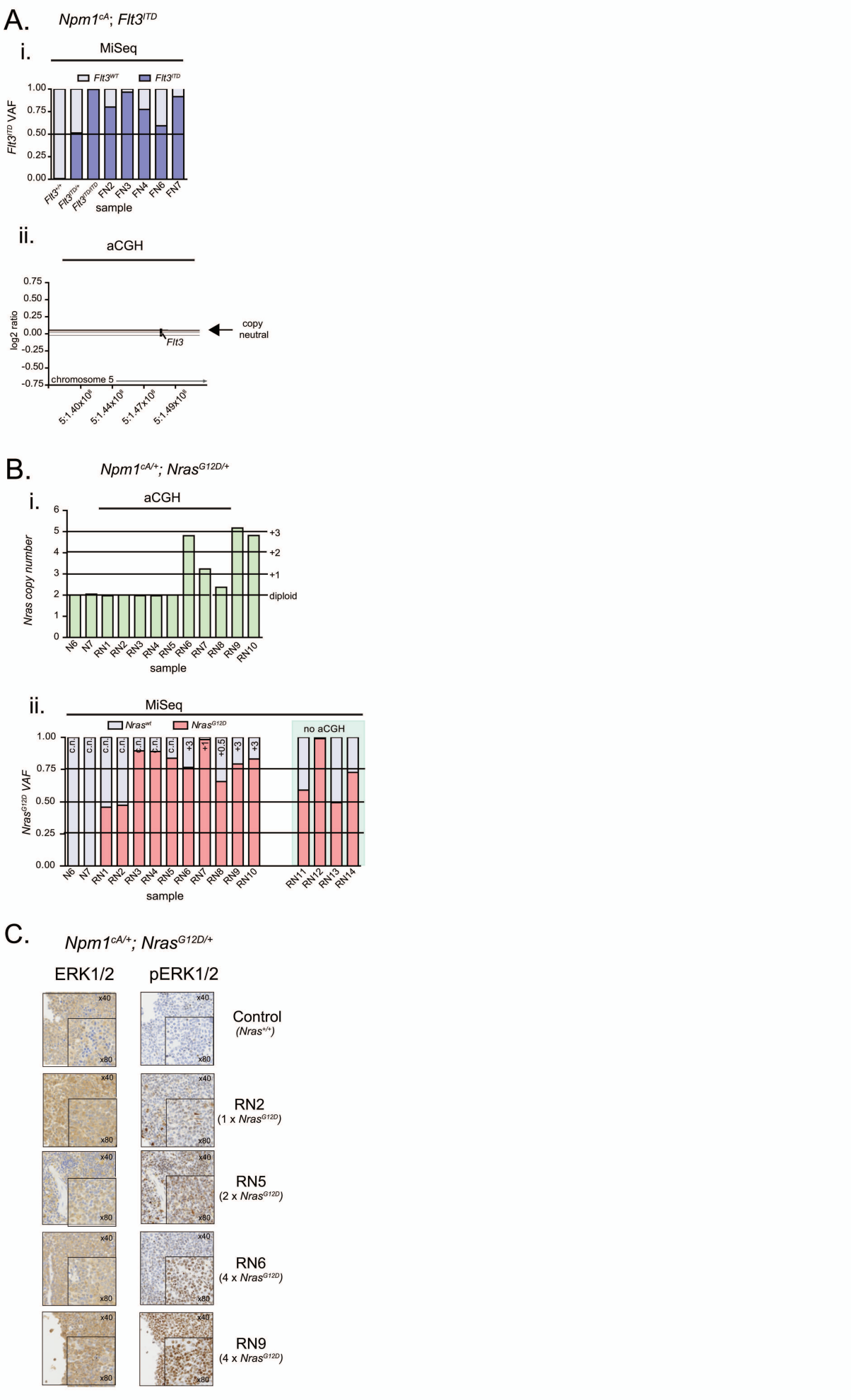

Figure 5

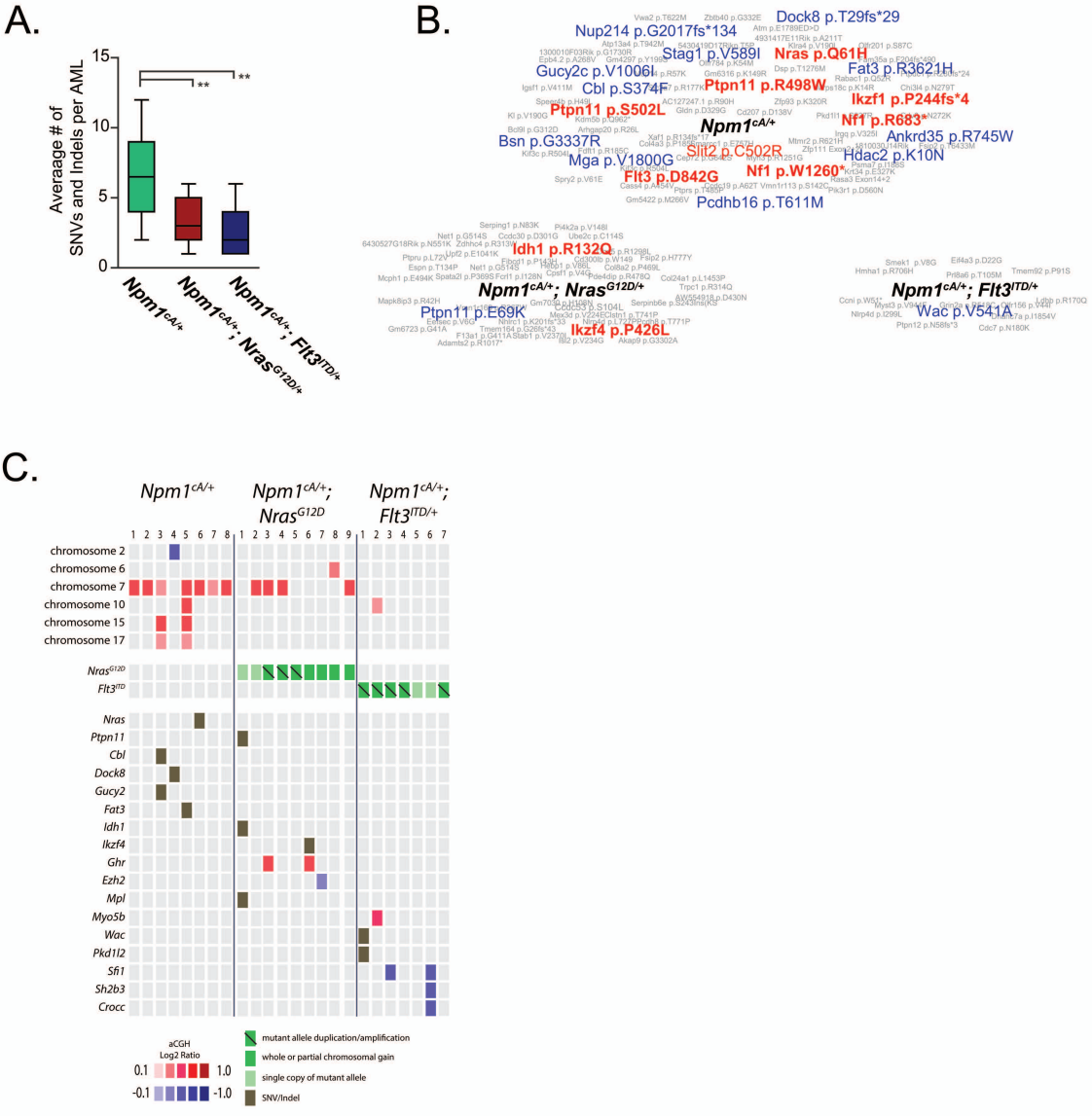
A.
Average # of SNVs and Indels per AML
15
10
5
0
**
**
Npm1cA/+
Npm1cA/+; NrasG12D/+
Npm1cA/+; Flt3ITD/+
B.
Dock8 p.T29fs*29
Nup214 p.G2017fs*134
Stag1 p.V589I
Nras p.Q61H
Gucy2c p.V1006I
Fat3 p.R3621H
Cbl p.S374F
Ptpn11 p.R498W
Ikzf1 p.P244fs*4
Ptpn11 p.S502L
Nf1 p.R683*
Npm1cA/+
Bsn p.G3337R
Ankrd35 p.R745W
Mga p.V1800G
Slit2 p.C502R
Hdac2 p.K10N
Nf1 p.W1260*
Flt3 p.D842G
Pcdhb16 p.T611M
Idh1 p.R132Q
Npm1cA/+; NrasG12D/+
Ptpn11 p.E69K
Ikzf4 p.P426L
Npm1cA/+; Flt3ITD/+
Wac p.V541A
C.
Npm1cA/+
Npm1cA/+; NrasG12D
Npm1cA/+; Flt3ITD/+
chromosome 2
chromosome 6
chromosome 7
chromosome 10
chromosome 15
chromosome 17
NrasG12D
Flt3ITD
Nras
Ptpn11
Cbl
Dock8
Gucy2
Fat3
Idh1
Ikzf4
Ghr
Ezh2
Mpl
Myo5b
Wac
Pkd1l2
Sfi1
Sh2b3
Crocc
aCGH Log2 Ratio
0.1
1.0
-0.1
-1.0
mutant allele duplication/amplification
whole or partial chromosomal gain
single copy of mutant allele
SNV/Indel

Figure 6

A.

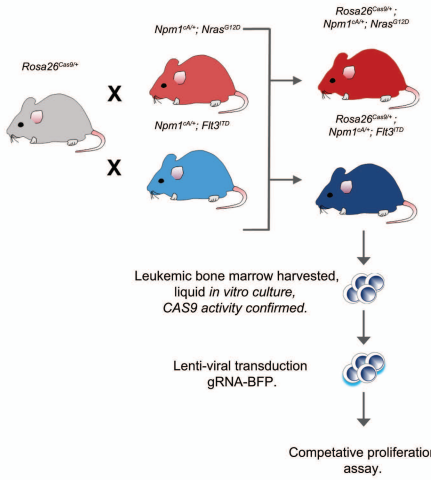
Rosa26Cas9/+
X
Npm1cA/+; NrasG12D
X
Npm1cA/+; Flt3ITD
Rosa26Cas9/+ ; Npm1cA/+; NrasG12D
Rosa26Cas9/+ ; Npm1cA/+; Flt3ITD
Leukemic bone marrow harvested, liquid in vitro culture, CAS9 activity confirmed.
Lenti-viral transduction gRNA-BFP.
Competative proliferation assay.

B.

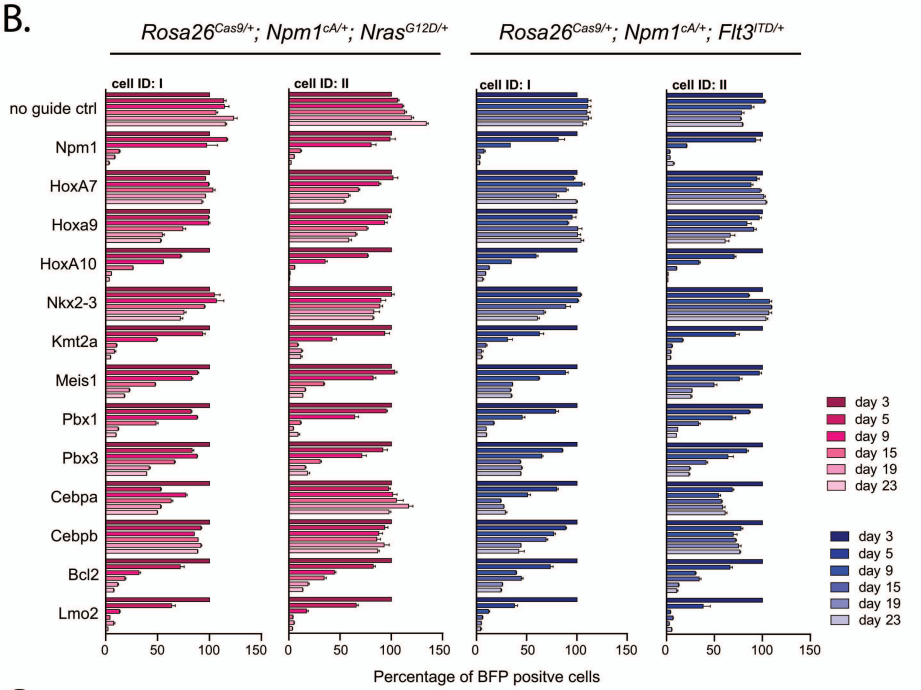
Rosa26Cas9/+; Npm1cA/+; NrasG12D/+
Rosa26Cas9/+; Npm1cA/+; Flt3ITD/+
cell ID: I
cell ID: II
cell ID: I
cell ID: II
no guide ctrl
Npm1
HoxA7
Hoxa9
HoxA10
Nkx2-3
Kmt2a
Meis1
Pbx1
Pbx3
Cebpa
Cebpb
Bcl2
Lmo2
0
50
100
150
day 3
day 5
day 9
day 15
day 19
day 23
Percentage of BFP positve cells

C.

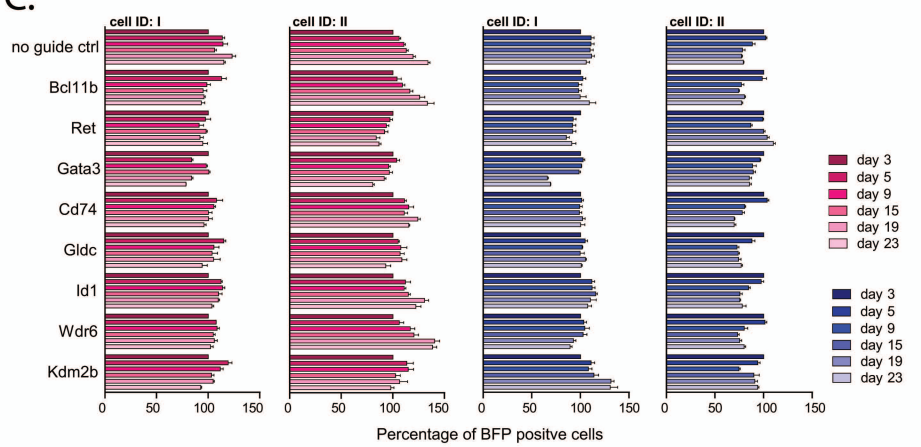
cell ID: I
cell ID: II
cell ID: I
cell ID: II
no guide ctrl
Bcl11b
Ret
Gata3
Cd74
Gldc
Id1
Wdr6
Kdm2b
0
50
100
150
day 3
day 5
day 9
day 15
day 19
day 23
Percentage of BFP positve cells

Prepublished online August 23, 2017;
doi:10.1182/blood-2017-01-760595

Molecular synergy underlies the co-occurrence patterns and phenotype of NPM1-mutant acute myeloid leukemia

Oliver M. Dovey, Jonathan L. Cooper, Annalisa Mupo, Carolyn S. Grove, Claire Lynn, Nathalie Conte, Robert M. Andrews, Suruchi Pacharne, Konstantinos Tzelepis, M.S. Vijayabaskar, Paul Green, Roland Rad, Mark Arends, Penny Wright, Kosuke Yusa, Allan Bradley, Ignacio Varela and George S. Vassiliou

Blood (print ISSN 0006-4971, online ISSN 1528-0020), is published weekly by the American Society of Hematology, 2021 L St, NW, Suite 900, Washington DC 20036.